ACS APPLIED MATERIALS & INTERFACES

www.acsami.org Research Article

Biomimetic Gradient Hydrogel Actuators with Ultrafast Thermo-Responsiveness and High Strength

Yuxi Li, Licheng Liu, Hao Xu, Zhihan Cheng, Jianhui Yan, and Xu-Ming Xie*

Cite This: ACS Appl. Mater. Interfaces 2022, 14, 32541−32550 Read Online

ACCESS | Metrics & More | Article Recommendations | Supporting Information

ABSTRACT: Most current hydrogel actuators suffer from either poor mechanical properties or limited responsiveness. Also, the widely used thermo-responsive poly-(*N*-isopropylacrylamide) (PNIPAM) homopolymer hydrogels have a slow response rate. Thus, it remains a challenge to fabricate thermo-responsive hydrogel actuators with both excellent mechanical and responsive properties. Herein, ultrafast thermo-responsive VSNPs-P(NIPAM-*co*-AA) hydrogels containing multivalent vinyl functionalized silica nanoparticles (VSNPs) are fabricated. The ultrafast thermo-responsiveness is due to the mobile polymer chains grafted from the surfaces of the VSNPs, which can facilitate hydrophobic aggregation, inducing the phase transition and generating water transport channels for quick water expulsion. In addition, the copolymerization of NIPAM with acrylic acid (AA) decreases the transition temperature of the thermo-responsive PNIPAM-based hydrogels, contributing to ultrafast thermo-responsive shrinking behavior with a large volume change of as high as 72.5%. Moreover, inspired by nature, intelligent hydrogel actuators with gradient structure can be facilely prepared through self-healing between the ultrafast thermo-responsive VSNPs-P(NIPAM-*co*-AA) hydrogel layers and high-strength VSNPs-PAA-Fe^{3+} multibond network (MBN) hydrogel layers. The obtained well-integrated gradient hydrogel actuators show ultrafast thermo-responsive performance within only 9 s in 60 °C water, as well as high strength, and can be used for more practical applications as intelligent soft actuators or artificial robots.

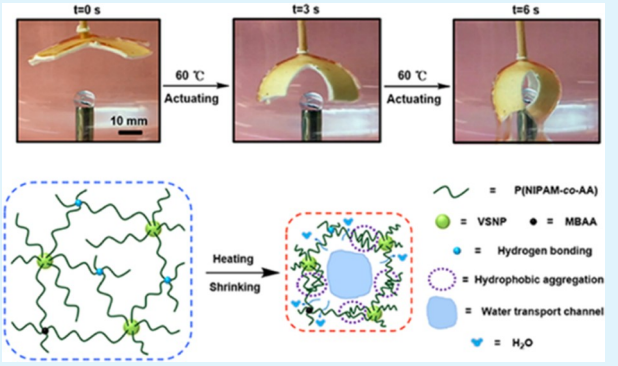

KEYWORDS: *biomimetic, gradient, hydrogel actuators, ultrafast thermo-responsiveness, high strength*

1. INTRODUCTION

In nature, most plants have an instinct gradient structure and can respond to external stimuli by hydration or dehydration of their cells,[1] or through a redistribution of water inside the tissues.[2] Inspired by the behaviors of natural plants, intelligent materials have been fabricated, which can generate deformations or movements according to external stimuli such as temperature,[3−5] humidity,[6] light,[7] pH,[8] chemicals, or solvents.[9,10] Among all of the artificial materials, hydrogels have a chemically or physically cross-linked three-dimensional polymeric network structure, which can absorb and retain a large amount of water and generate large deformations.[11] Therefore, flexible and intelligent hydrogel actuators have drawn a lot of attention and shown promising applications as biomedical devices and soft robots.[12,13] So far, numerous attempts have been made to create intelligent hydrogel actuators, such as via the introduction of responsive nanoparticles within hydrogels,[14,15] or through the fabrication of a bilayer hydrogel structure consisting of one responsive hydrogel layer and another nonresponsive substrate layer.[16−18] However, the common responsiveness or mechanical properties are still not enough for practical utilization.

Among various external stimuli, temperature can be easily applied and adjusted. One of the best known thermo-responsive polymers is poly-(*N*-isopropylacrylamide), namely PNIPAM.[19,20] Upon heating, the PNIPAM can go through a phase transition from hydration state to dehydration state in aqueous solution, possessing a lower critical solution temperature (LCST), also known as cloud point or phase transition temperature. Normally, the PNIPAM has an LCST of 31−33 °C in water.[21] The common PNIPAM homopolymer hydrogels are often chemically cross-linked by small molecules like *N*,*N*′-methylenebisacrylamide (MBAA). Once they are put into hot water with a temperature higher than the phase transition temperature, the PNIPAM homopolymer hydrogels will shrink gradually from the surface inwards and tend to form a collapsed, dense polymer skin layer at the surface. The dense polymer surface layer will inhibit further water permeation

Received: April 30, 2022
Accepted: June 28, 2022
Published: July 6, 2022

from the interior, and consequently, the response rate of the common PNIPAM homopolymer hydrogels is quite limited and slow.[22] By now, several strategies have been taken to improve the response rate of the thermo-responsive PNIPAM-based hydrogels, such as reducing the dimension of hydrogels,[23,24] introducing hydrophilic moieties to help with water transportation,[25,26] or incorporating mobile polymer chains to facilitate hydrophobic aggregation.[22,27] These approaches are able to improve the response rate of PNIPAM-based hydrogels to some extent, but the common responsive time scales are of minutes, which are yet not fast enough for practical applications such as intelligent soft actuators, flexible grippers, or soft robots. Besides, the thermo-responsive PNIPAM-based hydrogels often have a relatively low mechanical strength. Thus, it is still a great challenge to fabricate intelligent hydrogel actuators with both fast response rate and high strength.

Recently, based on the design of the multibond network (MBN), many tough and stretchable MBN hydrogels have been prepared.[28−45] In previous research, ionic nanocomposite VSNPs-PAA-Fe^{3+} physical hydrogels were constructed through a combination of multivalent vinyl functionalized silica nanoparticles (VSNPs) as "analogous covalent cross-linking", physical hydrogen bonds, and Fe^{3+}-mediated ionic interactions.[31] Under stretching, the rupture of the dynamic physical interactions could dissipate energy, giving rise to excellent mechanical properties. What's more, the reversible nature of the noncovalent ionic interactions and hydrogen bonds endowed the VSNPs-PAA-Fe^{3+} hydrogels with outstanding self-healing abilities.

In this work, involving multivalent VSNPs, thermo-responsive VSNPs-P(NIPAM-*co*-AA) hydrogels were synthesized via ultraviolet (UV) polymerization. The mobile polymer chains grafted from the surfaces of multivalent VSNPs are expected to facilitate hydrophobic aggregation upon heating, inducing the phase transition and generating water transport channels for quick water expulsion. Additionally, the copolymerization of NIPAM with AA can decrease the transition temperature (T_T) of the thermo-responsive PNIPAM-based hydrogels, and the larger supercooling degree may further accelerate the thermo-responsive shrinking rate. Furthermore, simply through self-healing between the fast thermo-responsive VSNPs-P(NIPAM-*co*-AA) hydrogel layers and strong VSNPs-PAA-Fe^{3+} MBN hydrogel layers, well-integrated gradient hydrogels can be fabricated. Hence, the obtained integrated gradient hydrogels with both fast thermo-responsiveness and high strength are promising to be used as thermo-responsive soft actuators.

2. EXPERIMENTAL SECTION

2.1. Materials. *N*-isopropylacrylamide (NIPAM) was provided by TCI Shanghai. Acrylic acid (AA) was purchased from Beijing Chemical Reagent Factory, purified by distillation under reduced pressure, and stored in a 4 °C refrigerator before usage. Vinyltriethoxysilane (VTES) and *N*,*N*′-methylenebisacrylamide (MBAA) were purchased from Acros Company. 2,2′-Azobis(2-methylpropionamidine) dihydrochloride (AIBA) was provided by J&K Chemicals Co., Ltd. Ferric chloride hexahydrate ($FeCl_3{\cdot}6H_2O$) was provided by Tianjin Jinke Institute of Fine Chemical Engineering. Deionized water with a resistivity of 18.2 MΩ cm at 25 °C was produced by a water purification system (GN-RO-100) and used throughout the experiments. All reagents were of analytical grade.

2.2. Preparation of the Vinyl Functionalized Silica Nanoparticles (VSNPs). As was described in the previous work,[29,32] a suspension with VSNPs in water was prepared using a universal sol−gel reaction. In a typical preparation process, VTES (1.0 g) and deionized water (8.0 g) were mixed, sealed, and put into a water-bath shaker with the power of 120 rpm at 25 °C. After 12 h, a transparent suspension with uniform dispersion of VSNPs in water was obtained. The average diameter of the VSNPs was around 3 nm through a transmission electron microscope measurement.[29]

2.3. Preparation of the Thermo-Responsive VSNPs-P(NIPAM-*co*-AA) Hydrogels. The thermo-responsive VSNPs-P(NIPAM-*co*-AA) hydrogels were prepared via a one-step ultraviolet polymerization. Typically, NIPAM and AA monomers (the whole monomer content was fixed at 20 wt %) as well as deionized water were uniformly mixed. Next, the VSNP suspension and MBAA (0.01 wt % relative to the whole monomer content) were added into the above mixture and dispersed under ultrasonic, obtaining a transparent and homogeneous mixture, which was later cooled down in an ice-water bath. Then, the AIBA photoinitiator aqueous solution (0.1 mol % to the whole monomer content) was added, mixed, and degassed under ultrasonic for 5 min. Afterward, the above uniform mixture was injected slowly into a pre-assembled mold (80 mm × 80 mm × 1 mm) made up of two pieces of transparent quartz glass and a silicone spacer. Later, the polymerization was carried out under ultraviolet irradiation (50 W power and 365 nm wavelength) in the ice-water bath for 3 h. After removal of the mold, the thermo-responsive VSNPs-P(NIPAM-*co*-AA) hydrogel was obtained, sealed, kept in a polyethylene bag, and stored in a 4 °C refrigerator. VSNPs-P(NIPAM-*co*-AA) hydrogels with different monomer ratios were prepared; to be specific, the molar ratio of NIPAM to AA was varied from 5:5, 6:4, 8:2 to 10:0. VSNPs-P(NIPAM-*co*-AA) hydrogels with different AA and VSNP contents were prepared. The VSNPs-P(NIPAM-*co*-AA) hydrogel is referred as "PN*x*A*y*-V*m*", where "N" and "A" represent NIPAM and AA, respectively, while "*x*" and "*y*" denote their corresponding molar ratios and "V" refers to VSNPs, with "*m*" being the concentration. Specifically, when the VSNP content is 0.5 wt % relative to the whole monomer weight, "PN*x*A*y*-V*m*" can be abbreviated as "PN*x*A*y*". For example, "PN6A4" stands for the VSNPs-P(NIPAM-*co*-AA) hydrogel whose monomer ratio of NIPAM to AA is 6 to 4 and VSNP content is 0.5 wt % of the whole monomer.

2.4. Preparation of the High-Strength VSNPs-PAA-Fe^{3+} Hydrogels. According to the recent research on the fabrication of tough ionic nanocomposite physical hydrogels,[29] the high-strength VSNPs-PAA-Fe^{3+} hydrogels were prepared through a simple one-pot *in situ* polymerization. Simply put, AA monomer (20 wt % relative to the hydrogel) and deionized water were uniformly mixed. Next, a VSNP suspension (0.5 wt % relative to AA) and $FeCl_3{\cdot}6H_2O$ (0.5 mol % relative to AA) were added into the above mixture and dispersed under ultrasonic, yielding a transparent and homogeneous mixture, which was later cooled down in an ice-water bath. Then, the AIBA photoinitiator aqueous solution (0.1 mol % to monomer AA) was added, mixed, and degassed under ultrasonic for 5 min. Later, the uniform suspension was injected slowly into a pre-assembled mold (80 mm × 80 mm × 1 mm) made up of two pieces of transparent quartz glass and a silicone spacer. Afterward, the polymerization was carried out under ultraviolet irradiation (50 W power and 365 nm wavelength) at room temperature for 3 h. After removal of the mold, the high-strength VSNPs-PAA-Fe^{3+} hydrogel was obtained, sealed, and stored in a polyethylene bag.

2.5. Fabrication of the Gradient Hydrogels. The gradient hydrogels were fabricated through self-healing between the thermo-responsive PNIPAM-based hydrogel layers and the high-strength VSNPs-PAA-Fe^{3+} hydrogel layers. To be specific, after the respective preparation of the thermo-responsive hydrogel layers and the high-strength hydrogel layers, they were then carefully stacked, sealed, and kept in a 4 °C environment for 24 h for adequate self-healing and integration.

2.6. Characterizations. *2.6.1. Determination of Volume Phase Transition Temperature (T_T) of the Thermo-Responsive Hydrogels.* The volume phase transition temperatures (T_T) of the thermo-responsive PNIPAM-based hydrogels were determined using the simplest, most convenient cloud point method.[21] The hydrogel

https://doi.org/10.1021/acsami.2c07631
ACS Appl. Mater. Interfaces 2022, 14, 32541−32550

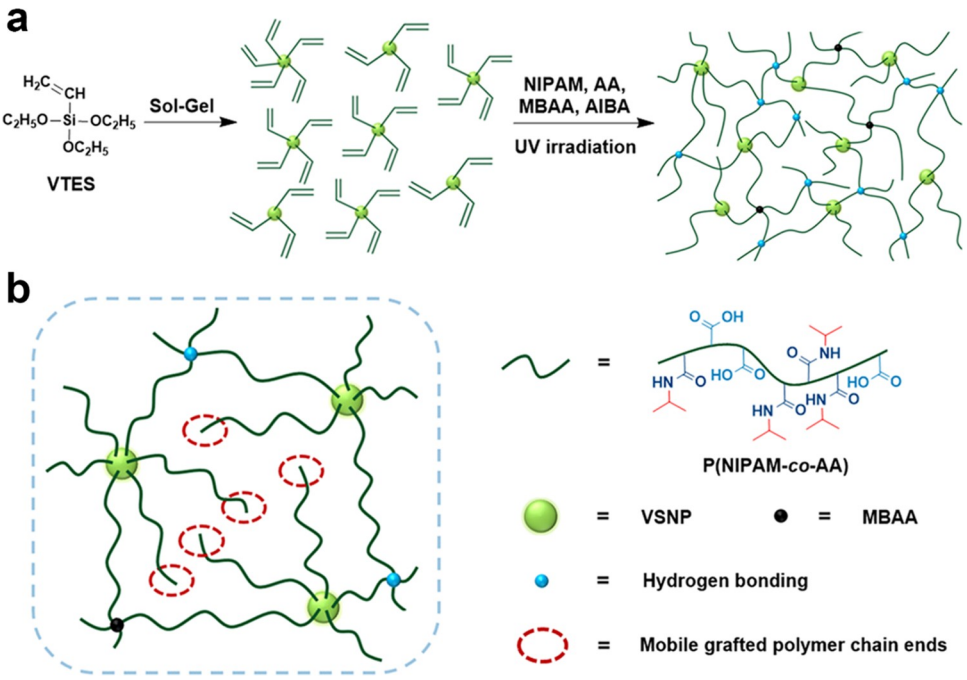

Figure 1. Thermo-responsive VSNPs-P(NIPAM-*co*-AA) hydrogels. (a) Synthesis and network structure of the hydrogels. The polymer network is constructed through the multivalent VSNPs (green balls), noncovalent hydrogen bonding (blue balls), and covalent cross-links by MBAA (black balls). AA monomer has carboxylic acid groups (in light blue), while NIPAM has both hydrophilic amide groups (in dark blue) and hydrophobic isopropyl groups (in red). (b) Schematic illustration of the mobile grafted polymer chain ends.

samples were first cut into 5 mm × 5 mm × 1 mm cuboids before testing, which were then put into heating stage and observed with a microscope. The temperature program was set from 4 to 40 °C, with a 1 °C min^{-1} heating rate and 5 min holding time at each temperature. The morphologies of the hydrogels at different temperatures were recorded by photographs. Upon heating, the thermo-responsive PNIPAM-based hydrogels underwent an obvious macroscopic phase separation change from transparent to opaque. The exact temperature at which the hydrogel went suddenly opaque was defined as its T_T (Figure S1).

2.6.2. Dynamic Shrinking Behaviors of the Thermo-Responsive Hydrogels. For the investigation of the dynamic volume-shrinking behaviors of the thermo-responsive PNIPAM-based hydrogels, the hydrogel film samples were precut into the size of 20 mm × 10 mm × 2 mm, then sealed and kept in a 4 °C refrigerator. During examination, these films were quickly immersed into a hot water bath. In the meantime, the real-time dynamic shrinking process of these hydrogel films was recorded with a digital camera. Afterward, the dimensions of the hydrogels at different times were measured from the digital photos intercepted from these videos. The shrinking degree in the length of the hydrogel is expressed as L/L_0, where L is the length of the hydrogel at some specific time during shrinking and L_0 is the initial length of the hydrogel sample; the value of L_0 is 20 mm in this case. For the thermo-responsive VSNPs-P(NIPAM-*co*-AA) hydrogels with different AA contents and varied VSNP concentrations, their shrinking degrees in length (L/L_0) in 60 °C water are plotted against time. In regard to each curve, the slope at the very beginning is defined as the response rate of the relative hydrogel.

In addition, dynamic shrinking behaviors of the PNIPAM-based hydrogels with different AA contents (VSNPs concentration was fixed at 0.5 wt %) in 50 and 40 °C water were also investigated and compared with the 60 °C measurement (Figure S2). Apparently, for each hydrogel, when the environmental temperature was higher, with a larger temperature difference as the external driving force, the thermo-responsive shrinking process became faster.

2.6.3. SEM Observation of the Gradient Hydrogels. Scanning electron microscopy (SEM) morphologies of the freeze-dried gradient hydrogels were observed by a tabletop SEM with Bruker XFlash detector 410-M. Before SEM observation, the gradient hydrogels were cut into small pieces and then frozen in liquid nitrogen for about 10 min. Afterward, they were lyophilized by a CHRIST Freeze Dryer for 48 h. The samples were sputtered with gold before observation and then visualized under a scanning electron microscope at an accelerating voltage of 10 kV.

2.6.4. Mechanical Measurements. For the measurements of the mechanical properties of the thermo-responsive PNIPAM-based hydrogels, hydrogel samples with the size of 40 mm × 10 mm × 2 mm were prepared, sealed, and kept in a 4 °C refrigerator. Uniaxial tensile measurements were carried out using a Shimadzu AGS-X universal testing machine at 10 °C temperature (below the transition temperatures of the thermo-responsive hydrogels), with the cross-head speed being 100 mm min^{-1} and the initial sample length between the jaws being 15 mm. During the test, the force applied on the hydrogel samples and the distance of deformation were recorded. Afterward, the tensile stress−strain curves were plotted, where stress σ was defined as the force applied on the hydrogel sample (F) divided by the initial cross-sectional area of the sample (A), that is $\sigma = F/A$, and strain ε was determined as the distance of deformation (Δx) divided by the initial gauge length (x_0), namely $\varepsilon = \Delta x/x_0$. Similarly, VSNPs-PAA-$Fe^{3+}$ hydrogel samples with the same size as above were made and tested under the same conditions. Also, the mechanical properties of the integrated gradient hydrogels were measured under the same testing parameters.

2.6.5. Demonstration of the Gradient Hydrogels as Thermo-Responsive Actuators. For the investigation of the thermo-responsive actuation behaviors of the gradient hydrogels, the gradient hydrogel integrated from the thermo-responsive VSNPs-PN6A4 hydrogel and the high-strength VSNPs-PAA-Fe^{3+} hydrogel was chosen. Then it was cut into cross-shaped grippers, sealed, and kept in a 4 °C refrigerator. During the experiments, these cross-shaped grippers were taken out and quickly put into a 60 °C hot water bath with some target objects inside, such as a transparent PMMA ball (0.1 g), a Miffy toy (0.5 g) made by ABS resin, and a PLA screw (1.0 g). Meanwhile, the real-time capture behaviors of these cross-shaped grippers were recorded by a digital camera (Videos S1, S2, and S3).

https://doi.org/10.1021/acsami.2c07631
ACS Appl. Mater. Interfaces 2022, 14, 32541−32550

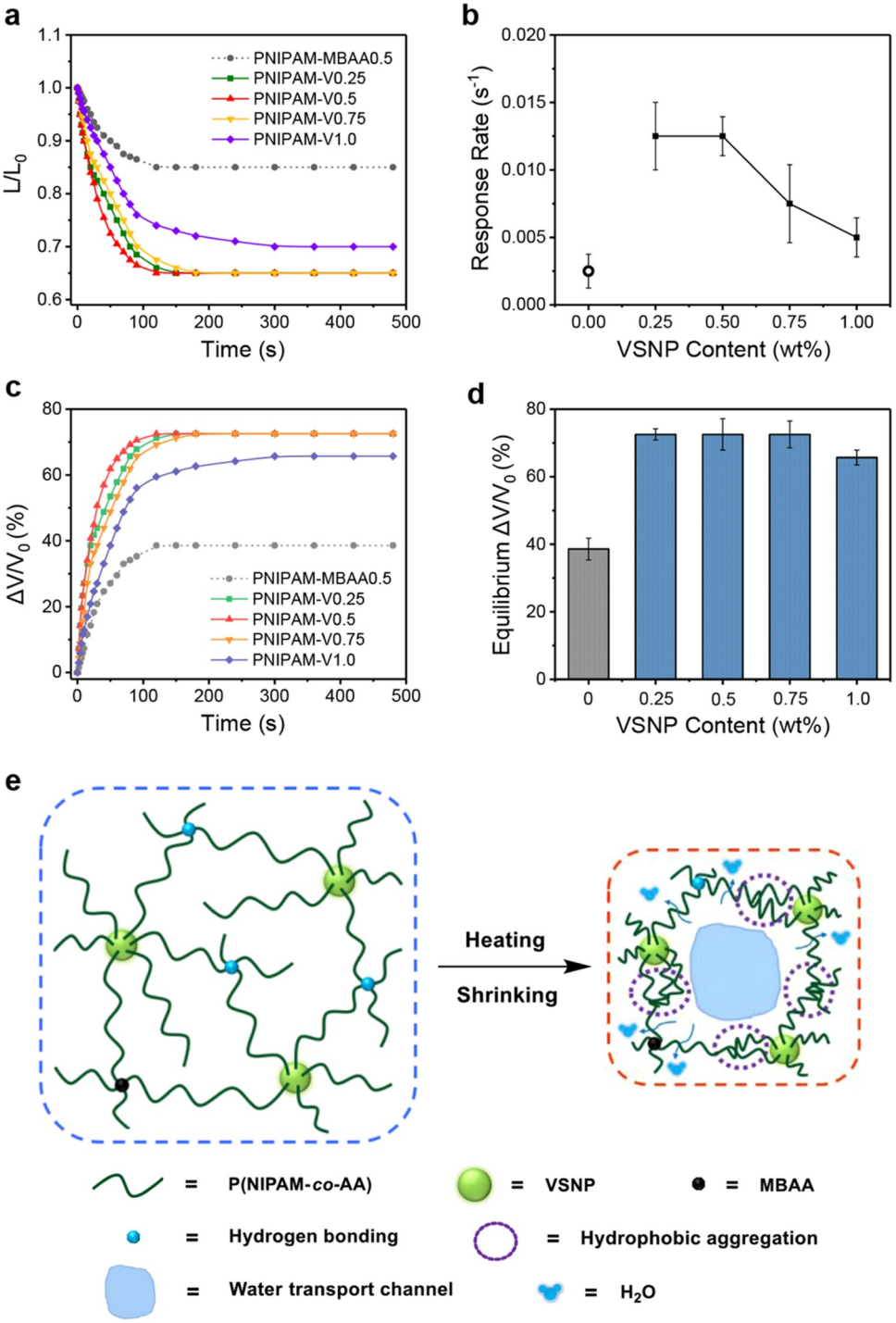

Figure 2. Thermo-responsive behaviors of the PNIPAM-based hydrogels composed of VSNPs. (a) Shrinking curves for length change (L/L_0) against time, (b) response rate, (c) volume shrinking ratio ($\Delta V/V_0$) against time, and (d) equilibrium volume shrinking ratio ($\Delta V/V_0$) of the PNIPAM hydrogels with varied VSNP contents in 60 °C water. (e) Illustration of the network structure transformation upon heating of the thermo-responsive PNIPAM-based hydrogels composed of VSNPs, showing the facilitated hydrophobic aggregation of the mobile grafted polymer chains, which can generate water transport channels inside the hydrogels and assist in quick water expulsion.

3. RESULTS AND DISCUSSION

3.1. Synthesis and Network Structure of the Thermo-Responsive VSNPs-P(NIPAM-*co*-AA) Hydrogels. Figure 1a shows clearly the synthesis and network structure of the thermo-responsive VSNPs-P(NIPAM-*co*-AA) hydrogels. Firstly, a suspension with VSNPs in water was prepared from vinyltriethoxysilane (VTES) by a universal sol−gel reaction. Then, through a simple UV polymerization, the thermo-responsive VSNPs-P(NIPAM-*co*-AA) hydrogels were synthesized by growing polymer chains from the initiated radicals on the surfaces of multivalent VSNPs under UV irradiation. As reported in the previous work, a series of nanocomposite hydrogels were prepared by grafting polymer chains from the surfaces of VSNPs through free-radical polymerization.[28−31] Here, in the reaction precursor of the thermo-responsive

https://doi.org/10.1021/acsami.2c07631
ACS Appl. Mater. Interfaces 2022, 14, 32541−32550

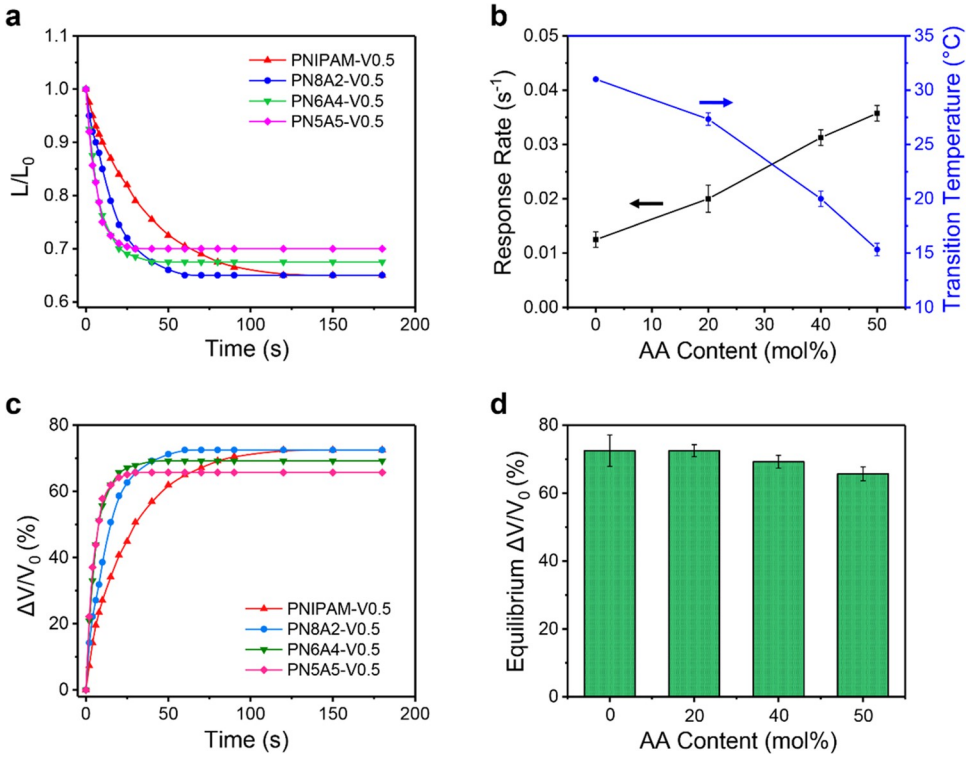

Figure 3. Thermo-responsive behaviors of the VSNPs-P(NIPAM-*co*-AA) hydrogels. (a) Shrinking curves for length change (L/L_0) against time, (b) response rate (black) and transition temperature (blue), (c) volume shrinking ratio ($\Delta V/V_0$) against time, and (d) equilibrium volume shrinking ratio ($\Delta V/V_0$) of the VSNPs-P(NIPAM-*co*-AA) hydrogels with varied AA contents in 60 °C water. VSNP contents are fixed at 0.5 wt %.

VSNPs-P(NIPAM-*co*-AA) hydrogels, the initiator tended to be adsorbed on the surfaces of VSNPs due to their large specific surface areas.[29,31] Under UV irradiation, the initiator would generate radicals, and free-radical polymerization was initiated at the vinyl groups on the surfaces of the VSNPs. The initiation and chain propagation from the surfaces of VSNPs could lead to the formation of grafted polymer chains with one terminus attached to one VSNP and the other hanging freely in water. The hydrogel network was constructed through multivalent VSNPs with grafted polymer chains like nano-brushes,[31] noncovalent hydrogen bonding, and covalent cross-links among polymer chains. As is shown in Figure 1b, the grafted P(NIPAM-*co*-AA) chains from the surfaces of VSNPs were relatively mobile with free chain ends, which could facilitate hydrophobic aggregation and thus induce volume phase transition upon heating, contributing to fast thermo-responsiveness. A detailed investigation of the network structure of hydrogels with grafted polymer chains was systematically discussed in the previous work.[28] The molecular weight of the grafted polymer chains was measured by gel permeation chromatography (GPC). Simply by varying the contents or diameters of the VSNPs, the length, density, and mobility of the grafted polymer chains could be easily adjusted. The existence and density of free chain ends of the hydrogels can be revealed based on the theory of rubber elasticity with tensile mechanical data, and the mobility of the grafted polymer chains can be confirmed by differential scanning calorimetry (DSC) measurements.[46,47] In addition, when pH < 4, the copolymerization of NIPAM with AA could enhance the attraction between the neighboring polymer chains through hydrogen bonding and decrease the T_T of the PNIPAM-based hydrogels.[19,20] These factors were able to improve the response rate of the thermo-responsive hydrogels.

3.2. Response Performance of the Thermo-Responsive VSNPs-P(NIPAM-*co*-AA) Hydrogels. To investigate the response performance of the thermo-responsive PNIPAM-based hydrogels with different VSNP contents, dynamic volume-shrinking behaviors of the hydrogel film samples were recorded in 60 °C water. Figure 2a shows the shrinking curves for length change versus time of the PNIPAM hydrogel films with varied VSNP contents, and Figure 2b shows their response rates calculated from the initial slopes of the shrinking curves in Figure 2a. Figure 2c,d displays the relevant volume shrinking ratio against time and the equilibrium volume shrinking ratio of PNIPAM hydrogels with varied VSNP contents, respectively. Obviously, in Figure 2a–d, the VSNP contents had a notable influence on the shrinking behaviors of the thermo-responsive PNIPAM-based hydrogels. In regard to the PNIPAM hydrogels chemically cross-linked by 0.5 wt % MBAA, both ends of the polymer chains were relatively constrained by the network and immobile. Thus, when immersed in hot water above the T_T, along with the expulsion of water, the hydrogel shrank gradually from the surface inwards, and a dense polymer skin layer tended to form at the surface, which would inhibit further water permeation from the interior. Consequently, the PNIPAM hydrogels cross-linked by 0.5 wt % MBAA showed a slow response rate at the very beginning (Figure 2a,b), and restricted the equilibrium volume shrinking ratio of only 38.6% to the original volume, shown in Figure 2c,d. By contrast, the hydrogels of VSNPs-PNIPAM containing 0.25–0.5 wt % VSNPs and only 0.01 wt % MBAA exhibited drastically increased initial response rates. The VSNPs-PNIPAM hydrogel network was constructed through the multivalent VSNPs with grafted polymer chains like nano-brushes,[31] and thus, the grafted polymer chains were relatively mobile with free chain ends. In this case, when the

https://doi.org/10.1021/acsami.2c07631
ACS Appl. Mater. Interfaces 2022, 14, 32541–32550

ambient temperature became higher than the T_T, the hydrogen bonds among polymer chains as well as those between polymer and water were disrupted. Then, the long and mobile grafted polymer chains could dehydrate easily and aggregate rapidly to form a hydrophobic aggregation, inducing the phase transition. Meanwhile, as illustrated in Figure 2e, the grafted polymer chains tended to curl up and form a hydrophobic aggregation around the relatively fixed multivalent VSNP cross-linking points, thus generating some water transport channels inside the hydrogels, which could assist in water expulsion. In addition, with multivalent VSNPs connecting the polymer network, the whole network would be dragged to collapse and squeeze out the entrapped water quickly through the water transport channels, contributing to the ultrafast thermo-responsive shrinking performance with a large equilibrium volume shrinking ratio of 72.5% relative to the original volume, as shown in Figure 2c,d. The introduction of grafted polymer chains into PNIPAM-based hydrogels has also been proven by others to increase the deswelling rate of the PNIPAM hydrogels, such as by copolymerization of NIPAM monomers with PNIPAM macromonomers,[22] by graft polymerization from the surfaces of microgels[27] or clay sheets.[46,47] Overall, the PNIPAM hydrogels with freely dangling polymer chains could shrink more rapidly, owing to their easier change in conformation, as for the flexible and mobile polymer chains. However, in regard to the VSNPs-PNIPAM hydrogels with more VSNPs of 0.75−1.0 wt %, the grafted polymer chains were shorter and less mobile;[29] therefore, the response behaviors became slower. Besides, a large number of VSNPs would cause a high cross-linking density in the VSNPs-PNIPAM hydrogels. As a consequence, due to the polymer chains with much more restricted mobility, the VSNPs-PNIPAM hydrogels composed of 1.0 wt % VSNPs possessed a slower response rate and smaller equilibrium volume shrinking ratio of 65.7% relative to the original volume.

Figure 3a shows the shrinking curves for length change versus time of the VSNPs-P(NIPAM-*co*-AA) hydrogel films containing different AA contents in 60 °C water with VSNPs fixed at 0.5 wt %. Figure 3b shows the response rates calculated from the initial slopes of the shrinking curves in Figure 3a. It is noteworthy that the copolymerization of NIPAM with AA could decrease the T_T of the PNIPAM-based hydrogels, which was decreased further with more copolymerized AA. The higher supercooling degree could generate a larger driving force for the phase transition of the VSNPs-P(NIPAM-*co*-AA) hydrogels. Therefore, along with the decrease in T_T, the initial response rates were observably improved, as shown in Figure 3b. The T_T was determined using the simplest, most convenient cloud point method (Figure S1). To be specific, the T_T of the VSNPs-PNIPAM hydrogels was 31 °C and that of the VSNPs-P(NIPAM-*co*-AA) hydrogels was decreased to 15 °C on increasing the copolymerized AA to 50 mol %. As is mentioned above, PNIPAM can go through a phase transition from the hydration state to the dehydration state in aqueous solution at T_T values of 31−33 °C upon heating.[21] By modifying the molecular structure, the T_T of the PNIPAM-based polymers can be changed.[19,20] In addition, as is confirmed by the volume shrinking ratio against time in Figure 3c, the VSNPs-P(NIPAM-*co*-AA) hydrogels consisting of a higher amount of AA presented much faster thermo-responsiveness. Moreover, it is worth mentioning that as for the VSNPs-P(NIPAM-*co*-AA) hydrogels with an original water content of 80 wt %, the water content was decreased to 50 wt % at a volume shrinking ratio of 60%. The decrease in water contents of the VSNPs-P(NIPAM-*co*-AA) hydrogels from 80 to 50 wt % implied the greatly improved tensile strength from 20 to 170 kPa, namely there was a self-enhancement in the mechanical properties during the thermo-responsive volume shrinking process (Figure S3). However, in regard to the equilibrium volume shrinking ratio relative to the AA contents shown in Figure 3d, the VSNPs-P(NIPAM-*co*-AA) hydrogels with more copolymerized AA had a slightly reduced volume shrinking ratio because there was a lesser number of thermo-responsive PNIPAM moieties in the VSNPs-P(NIPAM-*co*-AA) hydrogels.

3.3. Design and Actuating Mechanism, Mechanical, and Thermo-Responsive Properties of the Integrated Gradient Hydrogel Actuators.

Figure 4 demonstrates the design and actuating mechanism of the integrated gradient thermo-responsive hydrogel actuators. By means of self-healing between the thermo-responsive hydrogel layers and the high-strength hydrogel layers, integrated gradient hydrogels are facilely fabricated. Adequate self-healing can be realized by virtue of the reversible noncovalent interactions between different hydrogel layers. Then, because the different portions of the integrated gradient hydrogel actuators have different thermo-responsive volume transition behaviors, bending action can be achieved under the temperature stimulus. To be specific, when the surrounding temperature becomes higher than the T_T of the thermo-responsive PNIPAM-based hydrogel portions, they will go through obvious volume shrinking. By contrast, the nonresponsive VSNPs-PAA-Fe^{3+} hydrogel portions have no volume change. Thus, due to the difference in volume changes between the thermo-responsive and the high-strength hydrogel portions upon heating, the integrated gradient hydrogel actuators will bend towards the thermo-responsive PNIPAM-based hydrogel side. Based on the above design, biomimetic integrated gradient hydrogel actuators with fast thermo-responsiveness and high strength can be achieved, in which the fast thermo-responsive PNIPAM-based hydrogel portions on one side provide a rapid response rate and the strong VSNPs-PAA-Fe^{3+} hydrogel portions on the other side offer high strength.

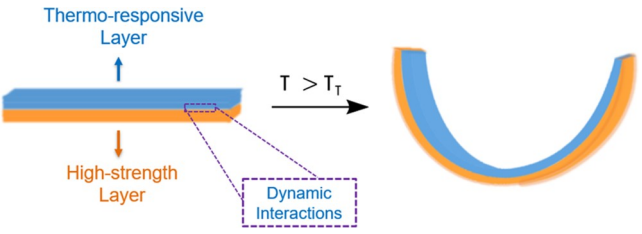

Figure 4. Design and actuating mechanism of the gradient thermo-responsive hydrogel actuators.

Through a simple UV polymerization, the high-strength VSNPs-PAA-Fe^{3+} MBN hydrogels were prepared by growing polymer chains from the initiated radicals on the surfaces of VSNPs. The hydrogel network was constructed with the VSNPs as multivalent cross-linking points, noncovalent hydrogen bonds, and Fe^{3+}-mediated ionic interactions among PAA chains. The VSNPs-PAA-Fe^{3+} hydrogels showed high strength owing to the rupture of the dynamic interactions for energy dissipation under stretching.[31] Moreover, the reversible hydrogen bonds and Fe^{3+}-mediated ionic interactions among

https://doi.org/10.1021/acsami.2c07631
ACS Appl. Mater. Interfaces 2022, 14, 32541−32550

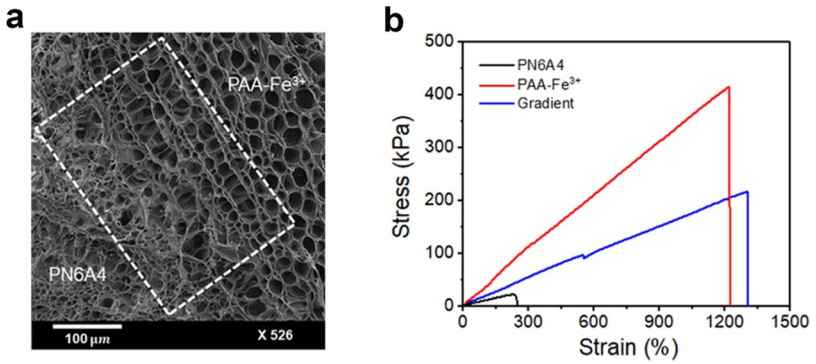

Figure 5. SEM micrograph and mechanical properties of the integrated gradient hydrogel composed of the thermo-responsive VSNPs-P(NIPAM-*co*-AA) hydrogel and the high-strength VSNPs-PAA-Fe^{3+} hydrogel. (a) SEM micrograph showing different porous microstructures and the dotted zone showing complete integration through self-healing with no obvious interface. (b) Tensile stress−strain curves of the thermo-responsive VSNPs-PN6A4 hydrogel, the VSNPs-PAA-Fe^{3+} hydrogel, and their integrated gradient hydrogel.

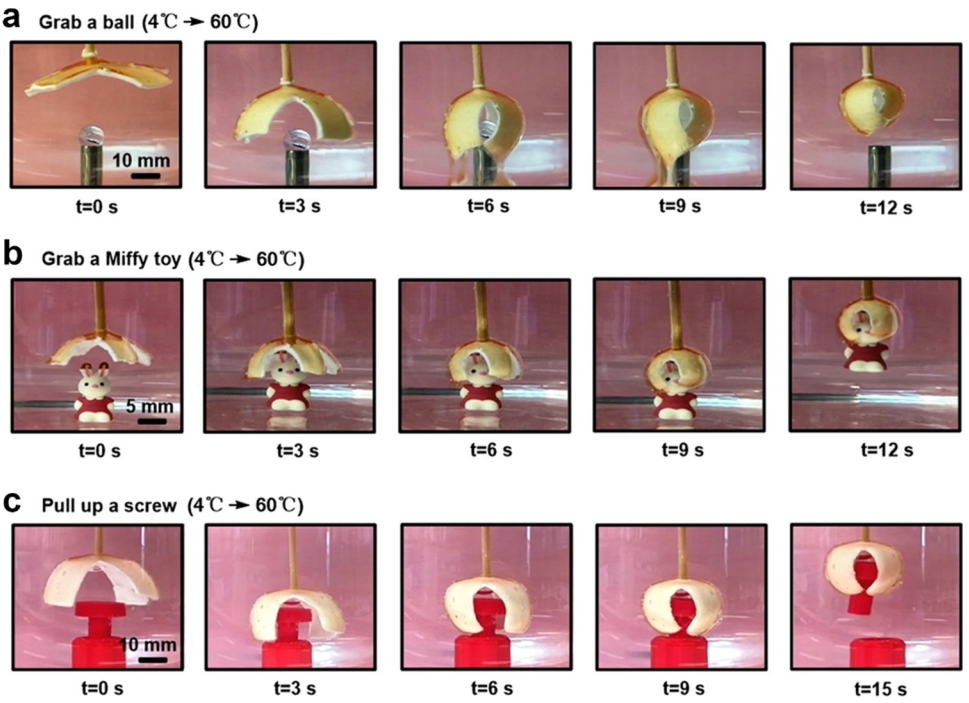

Figure 6. Schematic illustrations of the integrated gradient hydrogels as thermo-responsive grippers. (a) Grab a ball, (b) grab a Miffy toy, and (c) pull up a screw.

the PAA chains endowed the hydrogels with great self-healing abilities. Therefore, the hydrogels could be used to fabricate thermo-responsive gradient hydrogels by means of self-healing with the thermo-responsive PNIPAM-based hydrogels containing dynamic bonds, and thus, the obtained gradient hydrogels could be endowed with a high tensile strength as well.

Figure 5a shows the scanning electron microscopy (SEM) observation of the integrated gradient hydrogels. Clearly, the portions of the thermo-responsive VSNPs-PN6A4 and the strong VSNPs-PAA-Fe^{3+} in the gradient hydrogel exhibited different porous microstructures and they were well integrated through self-healing with no obvious interface. The excellent self-healing was ascribed to the dynamic hydrogen bonds and Fe^{3+}-mediated ionic interactions among the carboxyl groups in the polymer chains between different hydrogels. Especially, the diffusion of both the polymer chains and Fe^{3+} at the interface, and the recombination of these dynamic interactions were of great importance to the self-healing process, which could be enhanced by increasing the healing time and temperature.[31,38] On the contrary, many layered hydrogels combined through an interpenetrating network via layer-by-layer photopolymerization often have noticeable interfacial layers,[18] which are likely to separate during deformations or movements. Figure 5b compares the tensile stress−strain curves of the thermo-responsive VSNPs-PN6A4 hydrogel, the VSNPs-PAA-Fe^{3+} hydrogel, and their integrated gradient hydrogel. Obviously, the thermo-responsive VSNPs-PN6A4 hydrogel showed relatively poor mechanical properties with a tensile strength of no more than 30 kPa and small elongation at break. In contrast, the VSNPs-PAA-Fe^{3+} hydrogel had excellent mechanical properties with a high tensile strength of 400 kPa and a large elongation at break of 1250%. This is attributed to the dynamic dissociation of hydrogen bonds and Fe^{3+}-mediated ionic interactions under stretching to dissipate energy, and VSNPs acting as multivalent cross-linking points

https://doi.org/10.1021/acsami.2c07631
ACS Appl. Mater. Interfaces 2022, 14, 32541−32550

to maintain the hydrogel network. After complete integration through self-healing between the thermo-responsive VSNPs-PN6A4 hydrogel and the strong VSNPs-PAA-Fe^{3+} hydrogel, the obtained integrated gradient hydrogel exhibited a high tensile strength of 250 kPa as well as a large elongation at break of 1300%. Here, it needs to be mentioned that during stretching, the weaker thermo-responsive hydrogel portion with a shorter elongation at break would fracture before the overall breaking of the integrated gradient hydrogel. But, as shown in Figure 5b, the small break at around 600% of the integrated gradient hydrogel was much larger than the elongation at break of 230% for the weaker hydrogel layer. Both the improvement in the strength and stretchability indicated the synergistic effect and good integration of the gradient hydrogels and effective mechanical strengthening from the strong VSNPs-PAA-Fe^{3+} hydrogel. The elongation of 600% was enough for many application situations. Besides, although there was a small break at around 600% as a consequence of the partial break of the weaker thermo-responsive hydrogel, the thermo-responsive hydrogel and strong hydrogel were still nicely integrated during the whole tensile test without any observed separation at the interface. That is, even when the gradient hydrogel was fractured, the interfacial area was still strongly adhered, indicating the complete integration through self-healing with strong and stable interfacial adhesion. Therefore, the integrated gradient hydrogels with great mechanical properties are promising for more practical applications, like soft robots and flexible actuators.

Figure 6 demonstrates the application of the integrated gradient hydrogels as thermo-responsive soft actuators, which are obtained through self-healing between the thermo-responsive VSNPs-PN6A4 hydrogels and the high-strength VSNPs-PAA-Fe^{3+} hydrogels. Before testing, the integrated gradient hydrogels were cut into cross-shaped grippers. Once transferred from 4 °C into 60 °C water, much higher than the T_T of 20 °C for the thermo-responsive VSNPs-PN6A4 hydrogels, these cross-shaped gradient hydrogel grippers immediately started to bend and curl up with a large bending degree. Therefore, the hydrogel grippers were able to wrap and capture items, such as a transparent ball, a Miffy toy, and a screw, with an ultrafast performance of ∼9 s (Videos S1, S2, and S3). In addition, after 9 s in 60 °C water, the VSNPs-PN6A4 hydrogels with decreased water contents from 80 to 50 wt % exhibited greatly enhanced tensile strength (Figures 3c and S3). Therefore, the integrated gradient hydrogel grippers containing the thermo-responsive hydrogels with self-enhanced mechanical properties were able to robustly encapsulate and grab much heavier items than many other reported hydrogel actuators.[17,18] What's more, with ultrafast thermo-responsive actuating performance at time scales of seconds, the integrated gradient hydrogel actuators outperform most current hydrogel actuators, which often need several minutes to respond and actuate.[17,18] Even though, by generating a large porous structure inside the thermo-responsive PNIPAM-based hydrogels, the response rate can be improved,[16,24] the preparation process is complicated, tedious, and in requirement for some pore-forming agents. Besides, the PNIPAM-based hydrogels with a large porous structure often exhibit a relatively low mechanical strength, which is a distinct disadvantage for their application as durable actuators. In comparison, simply through self-healing between the fast thermo-responsive hydrogels and the high-strength hydrogels, it is facile and time saving to fabricate the integrated gradient hydrogel actuators. Moreover, owing to the VSNPs with mobile grafted polymer chains facilitating hydrophobic aggregation and quick water expulsion in the thermo-responsive hydrogels, as well as enhanced mechanical strength from the tough VSNPs-PAA-Fe^{3+} hydrogels, the obtained integrated gradient hydrogel actuators possess ultrafast thermo-responsiveness and high strength, and are much more promising to be used as practical intelligent flexible actuators or soft robots.

4. CONCLUSIONS

Biomimetic intelligent gradient hydrogel actuators with both ultrafast thermo-responsiveness and high strength were designed and fabricated in this work. Because of containing multivalent VSNPs, the synthesized thermo-responsive VSNPs-P(NIPAM-*co*-AA) hydrogels had an ultrafast response rate, in that the mobile polymer chains grafted from the surfaces of VSNPs could facilitate hydrophobic aggregation and quick water expulsion. In addition, the copolymerization of NIPAM with AA decreased the transition temperature of the thermo-responsive PNIPAM-based hydrogels, contributing to the ultrafast thermo-responsive shrinking performance with large volume shrinking ratios of up to 72.5%. Moreover, through self-healing between the ultrafast thermo-responsive VSNPs-P(NIPAM-*co*-AA) hydrogels and strong VSNPs-PAA-Fe^{3+} MBN hydrogels, well-integrated gradient hydrogels were facilely fabricated. The obtained integrated gradient hydrogels showed ultrafast thermo-responsiveness within only 9 s and a high tensile strength of 250 kPa, and hence could be used for more practical applications such as intelligent flexible actuators or soft robots.

■ ASSOCIATED CONTENT

Supporting Information

The Supporting Information is available free of charge at https://pubs.acs.org/doi/10.1021/acsami.2c07631.

Optical pictures for the determination of transition temperature; mechanical properties; dynamic shrinking and swelling curves; thermo-responsive bending behaviors (PDF)

Video S1: real-time video of a cross-shaped gradient hydrogel gripper to grab a transparent PMMA ball (0.1 g) in 60 °C water (MP4)

Video S2: real-time video of a cross-shaped gradient hydrogel gripper to grab a Miffy toy (0.5 g) in 60 °C water (MP4)

Video S3: real-time video of a cross-shaped gradient hydrogel gripper to pull up a PLA screw (1.0 g) in 60 °C water (MP4)

■ AUTHOR INFORMATION

Corresponding Author

Xu-Ming Xie − *Key Laboratory of Advanced Materials (MOE), Department of Chemical Engineering, Tsinghua University, Beijing 100084, China;* orcid.org/0000-0003-3344-7856; Email: xxm-dce@mail.tsinghua.edu.cn

Authors

Yuxi Li − *Key Laboratory of Advanced Materials (MOE), Department of Chemical Engineering, Tsinghua University, Beijing 100084, China;* orcid.org/0000-0001-7814-1709

Licheng Liu − *Key Laboratory of Advanced Materials (MOE), Department of Chemical Engineering, Tsinghua University, Beijing 100084, China*
Hao Xu − *Key Laboratory of Advanced Materials (MOE), Department of Chemical Engineering, Tsinghua University, Beijing 100084, China*
Zhihan Cheng − *Key Laboratory of Advanced Materials (MOE), Department of Chemical Engineering, Tsinghua University, Beijing 100084, China*
Jianhui Yan − *Key Laboratory of Advanced Materials (MOE), Department of Chemical Engineering, Tsinghua University, Beijing 100084, China*

Complete contact information is available at: https://pubs.acs.org/10.1021/acsami.2c07631

Author Contributions

Y.L. and X.-M.X. conceived and designed the experiments. Y.L. and L.L. conducted the hydrogel synthesis, and mechanical and thermo-responsive measurements. Z.C. carried out the SEM measurement. Y.L. and X.-M.X. analyzed the data and co-wrote the paper. All authors discussed the results and commented on the manuscript.

Funding

The authors acknowledge the National Natural Science Foundation of China (Nos. 21774069, 51633003, and 21474058) for financial support.

Notes

The authors declare no competing financial interest.

REFERENCES

(1) Armon, S.; Efrati, E.; Kupferman, R.; Sharon, E. Geometry and Mechanics in the Opening of Chiral Seed Pods. *Science* **2011**, *333*, 1726−1730.
(2) Dumais, J.; Forterre, Y. "Vegetable Dynamicks": The Role of Water in Plant Movements. *Annu. Rev. Fluid Mech.* **2012**, *44*, 453−478.
(3) Zhang, L.; Desta, I.; Naumov, P. Synergistic Action of Thermoresponsive and Hygroresponsive Elements Elicits Rapid and Directional Response of a Bilayer Actuator. *Chem. Commun.* **2016**, *52*, 5920−5923.
(4) Ma, C.; Le, X.; Tang, X.; He, J.; Xiao, P.; Zheng, J.; Xiao, H.; Lu, W.; Zhang, J.; Huang, Y.; Chen, T. A Multiresponsive Anisotropic Hydrogel with Macroscopic 3D Complex Deformations. *Adv. Funct. Mater.* **2016**, *26*, 8670−8676.
(5) Liu, Y.; Zhang, K.; Ma, J.; Vancso, G. J. Thermoresponsive Semi-IPN Hydrogel Microfibers from Continuous Fluidic Processing with High Elasticity and Fast Actuation. *ACS Appl. Mater. Interfaces* **2017**, *9*, 901−908.
(6) Kuang, Y.; Chen, C.; Cheng, J.; Pastel, G.; Li, T.; Song, J.; Jiang, F.; Li, Y.; Zhang, Y.; Jang, S.; Chen, G.; Li, T.; Hu, L. Selectively Aligned Cellulose Nanofibers towards High-Performance Soft Actuators. *Extreme Mech. Lett.* **2019**, *29*, No. 100463.
(7) Wang, H.; Liu, Z.; Liu, Z.; Jiang, J.; Li, G. Photo-Dissociable Fe^{3+}-Carboxylate Coordination: A General Approach toward Hydrogels with Shape Programming and Active Morphing Functionalities. *ACS Appl. Mater. Interfaces* **2021**, *13*, 59310−59319.
(8) Zhuo, J.; Wu, B.; Zhang, J.; Peng, Y.; Lu, H.; Le, X.; Wei, S.; Chen, T. Supramolecular Assembly of Shape Memory and Actuating Hydrogels for Programmable Shape Transformation. *ACS Appl. Mater. Interfaces* **2022**, *14*, 3551.
(9) Xu, T.; Han, Q.; Cheng, Z.; Zhang, J.; Qu, L. Interactions between Graphene-Based Materials and Water Molecules toward Actuator and Electricity-Generator Applications. *Small Methods* **2018**, *2*, No. 1800108.
(10) Wang, L.; Liu, F.; Qian, J.; Wu, Z.; Xiao, R. Multi-Responsive PNIPAM−PEGDA Hydrogel Composite. *Soft Matter* **2021**, *17*, 10421−10427.
(11) Ahmed, E. M. Hydrogel: Preparation, Characterization, and Applications: A Review. *J. Adv. Res.* **2015**, *6*, 105−121.
(12) Sano, K.; Ishida, Y.; Aida, T. Synthesis of Anisotropic Hydrogels and Their Applications. *Angew. Chem., Int. Ed.* **2018**, *57*, 2532−2543.
(13) Le, X.; Lu, W.; Zhang, J.; Chen, T. Recent Progress in Biomimetic Anisotropic Hydrogel Actuators. *Adv. Sci.* **2019**, *6*, No. 1801584.
(14) Wei, X.; Chen, L.; Wang, Y.; Sun, Y.; Ma, C.; Yang, X.; Jiang, S.; Duan, G. An Electrospinning Anisotropic Hydrogel with Remotely-Controlled Photo-Responsive Deformation and Long-Range Navigation for Synergist Actuation. *Chem. Eng. J.* **2022**, *433*, No. 134258.
(15) Wu, L.; Ohtani, M.; Takata, M.; Saeki, A.; Seki, S.; Ishida, Y.; Aida, T. Magnetically Induced Anisotropic Orientation of Graphene Oxide Locked by *in situ* Hydrogelation. *ACS Nano* **2014**, *8*, 4640−4649.
(16) Jian, Y.; Wu, B.; Yang, X.; Peng, Y.; Zhang, D.; Yang, Y.; Qiu, H.; Lu, H.; Zhang, J.; Chen, T. Stimuli-Responsive Hydrogel Sponge for Ultrafast Responsive Actuator. *Supramol. Mater.* **2022**, *1*, No. 100002.
(17) Zheng, J.; Xiao, P.; Le, X.; Lu, W.; Théato, P.; Ma, C.; Du, B.; Zhang, J.; Huang, Y.; Chen, T. Mimosa Inspired Bilayer Hydrogel Actuator Functioning in Multi-Environments. *J. Mater. Chem. C* **2018**, *6*, 1320−1327.
(18) Ma, C.; Lu, W.; Yang, X.; He, J.; Le, X.; Wang, L.; Zhang, J.; Serpe, M. J.; Huang, Y.; Chen, T. Bioinspired Anisotropic Hydrogel Actuators with On−Off Switchable and Color-Tunable Fluorescence Behaviors. *Adv. Funct. Mater.* **2018**, *28*, No. 1704568.
(19) Nakayama, M.; Okano, T. Intelligent Thermoresponsive Polymeric Micelles for Targeted Drug Delivery. *J. Drug Delivery Sci. Technol.* **2006**, *16*, 35−44.
(20) Khan, A. Preparation and Characterization of N-isopropylacrylamide/Acrylic Acid Copolymer Core−Shell Microgel Particles. *J. Colloid Interface Sci.* **2007**, *313*, 697−704.
(21) Schild, H. G. Poly(N-isopropylacrylamide): Experiment, Theory and Application. *Prog. Polym. Sci.* **1992**, *17*, 163−249.
(22) Yoshida, R.; Uchida, K.; Kaneko, Y.; Sakai, K.; Kikuchi, A.; Sakurai, Y.; Okano, T. Comb-Type Grafted Hydrogels with Rapid Deswelling Response to Temperature Changes. *Nature* **1995**, *374*, 240−242.
(23) Li, Y.; Guo, H.; Gan, J.; Zheng, J.; Zhang, Y.; Wu, K.; Lu, M. Novel Fast Thermal-Responsive Poly(N-isopropylacrylamide) Hydrogels with Functional Cyclodextrin Interpenetrating Polymer Networks for Controlled Drug Release. *J. Polym. Res.* **2015**, *22*, 1−14.
(24) Pan, Y.; Li, B.; Liu, Z.; Yang, Z.; Yang, X.; Shi, K.; Li, W.; Peng, C.; Wang, W.; Ji, X. Superfast and Reversible Thermoresponse of Poly(N-isopropylacrylamide) Hydrogels Grafted on Macroporous Poly(Vinyl Alcohol) Formaldehyde Sponges. *ACS Appl. Mater. Interfaces* **2018**, *10*, 32747−32759.
(25) Kaneko, Y.; Nakamura, S.; Sakai, K.; Aoyagi, T.; Kikuchi, A.; Sakurai, Y.; Okano, T. Rapid Deswelling Response of Poly(N-isopropylacrylamide) Hydrogels by the Formation of Water Release Channels Using Poly(Ethylene Oxide) Graft Chains. *Macromolecules* **1998**, *31*, 6099−6105.
(26) Zhao, Y.; Ju, X. J.; Zhang, L. P.; Wang, W.; Faraj, Y.; Zou, L. B.; Xie, R.; Liu, Z.; Chu, L. Y. Transparent Thermo-Responsive Poly(N-isopropylacrylamide)-l-Poly(Ethylene Glycol) Acrylamide Conetwork Hydrogels with Rapid Deswelling Response. *New J. Chem.* **2019**, *43*, 9507−9515.
(27) Xia, L. W.; Ju, X. J.; Liu, J. J.; Xie, R.; Chu, L. Y. Responsive Hydrogels with Poly(N-isopropylacrylamide-co-Acrylic Acid) Colloidal Spheres as Building Blocks. *J. Colloid Interface Sci.* **2010**, *349*, 106−113.
(28) Yang, J.; Shi, F. K.; Gong, C.; Xie, X. M. Dual Cross-Linked Networks Hydrogels with Unique Swelling Behavior and High

Mechanical Strength: Based on Silica Nanoparticle and Hydrophobic Association. *J. Colloid Interface Sci.* **2012**, *381*, 107−115.
(29) Shi, F. K.; Wang, X. P.; Guo, R. H.; Zhong, M.; Xie, X. M. Highly Stretchable and Super Tough Nanocomposite Physical Hydrogels Facilitated by the Coupling of Intermolecular Hydrogen Bonds and Analogous Chemical Crosslinking of Nanoparticles. *J. Mater. Chem. B* **2015**, *3*, 1187−1192.
(30) Huang, Y.; Zhong, M.; Huang, Y.; Zhu, M. S.; Pei, Z. X.; Wang, Z. F.; Xue, Q.; Xie, X. M.; Zhi, C. Y. A Self-Healable and Highly Stretchable Supercapacitor Based on a Dual Crosslinked Polyelectrolyte. *Nat. Commun.* **2015**, *6*, No. 10310.
(31) Zhong, M.; Liu, X. Y.; Shi, F. K.; Zhang, L. Q.; Wang, X. P.; Cheetham, A. G.; Cui, H.; Xie, X. M. Self-Healable, Tough and Highly Stretchable Ionic Nanocomposite Physical Hydrogels. *Soft Matter* **2015**, *11*, 4235−4241.
(32) Zhong, M.; Liu, Y. T.; Xie, X. M. Self-Healable, Super Tough Graphene Oxide-Poly(Acrylic Acid) Nanocomposite Hydrogels Facilitated by Dual Cross-Linking Effects through Dynamic Ionic Interactions. *J. Mater. Chem. B* **2015**, *3*, 4001−4008.
(33) Zhang, L. Q.; Chen, L. W.; Zhong, M.; Shi, F. K.; Liu, X. Y.; Xie, X. M. Phase Transition Temperature Controllable Poly-(Acrylamide-co-Acrylic Acid) Nanocomposite Physical Hydrogels with High Strength. *Chin. J. Polym. Sci.* **2016**, *34*, 1261−1269.
(34) Shi, F. K.; Zhong, M.; Zhang, L. Q.; Liu, X. Y.; Xie, X. M. Robust and Self-Healable Nanocomposite Physical Hydrogel Facilitated by the Synergy of Ternary Crosslinking Points in a Single Network. *J. Mater. Chem. B* **2016**, *4*, 6221−6227.
(35) Zhong, M.; Liu, Y. T.; Liu, X. Y.; Shi, F. K.; Zhang, L. Q.; Zhu, M. F.; Xie, X. M. Dually Cross-Linked Single Network Poly(Acrylic Acid) Hydrogels with Superior Mechanical Properties and Water Absorbency. *Soft Matter* **2016**, *12*, 5420.
(36) Huang, Y.; Zhong, M.; Shi, F. K.; Liu, X. Y.; Tang, Z. J.; Wang, Y. K.; Huang, Y.; Hou, H. Q.; Xie, X. M.; Zhi, C. Y. An Intrinsically Stretchable and Compressible Supercapacitor Containing a Polyacrylamide Hydrogel Electrolyte. *Angew. Chem., Int. Ed.* **2017**, *56*, 9141−9145.
(37) Shi, F. K.; Zhong, M.; Zhang, L. Q.; Liu, X. Y.; Xie, X. M. Toughening Mechanism of Nanocomposite Physical Hydrogels Fabricated by a Single Gel Network with Dual Crosslinking−The Roles of the Dual Crosslinking Points. *Chin. J. Polym. Sci.* **2017**, *35*, 25−35.
(38) Liu, X. Y.; Zhong, M.; Shi, F. K.; Xu, H.; Xie, X. M. Multi-Bond Network Hydrogels with Robust Mechanical and Self-Healable Properties. *Chin. J. Polym. Sci.* **2017**, *35*, 1253−1267.
(39) Liu, X. Y.; Xu, H.; Xie, X. M.; et al. Homogeneous and Real Super Tough Multi-Bond Network Hydrogels Created through a Controllable Metal Ion Permeation Strategy. *ACS Appl. Mater. Interfaces* **2019**, *11*, 42856−42864.
(40) Xu, H.; Shi, F. K.; Liu, X. Y.; Zhong, M.; Xie, X. M. How Can Multi-Bond Network Hydrogels Dissipate Energy More Effectively: An Investigation on the Relationship between Network Structure and Properties. *Soft Matter* **2020**, *16*, 4407.
(41) Fan, C.; Liu, B.; Xu, Z.; Cui, C.; Wu, T.; Yang, Y.; Liu, W.; et al. Polymerization of N-Acryloylsemicarbazide: A Facile and Versatile Strategy to Tailor-Make Highly Stiff and Tough Hydrogels. *Mater. Horiz.* **2020**, *7*, 1160−1170.
(42) Du, C.; Zhang, X. N.; Sun, T. L.; Du, M.; Zheng, Q.; Wu, Z. L. Hydrogen-Bond Association-Mediated Dynamics and Viscoelastic Properties of Tough Supramolecular Hydrogels. *Macromolecules* **2021**, *54*, 4313−4325.
(43) Xu, H.; Xie, X. M. Super-Tough and Rapidly Self-Recoverable Multi-Bond Network Hydrogels Facilitated by 2-Ureido-4[1H]-Pyrimidone Dimers. *Chin. Chem. Lett.* **2021**, *32*, 521−524.
(44) Li, Y.; Yan, J.; Liu, Y.; Xie, X. M. Super Tough and Intelligent Multibond Network Physical Hydrogels Facilitated by $Ti_3C_2T_x$ MXene Nanosheets. *ACS Nano* **2022**, *16*, 1567−1577.
(45) Xu, H.; Liu, Y. J.; Xie, X. M. Stretchable Alkaline Quasi-Solid-State Electrolytes Created by Super-Tough, Fatigue-Resistant and Alkali-Resistant Multi-Bond Network Hydrogels. *Chin. Chem. Lett.* **2022**, DOI: 10.1016/j.cclet.2022.04.068.
(46) Haraguchi, K.; Takehisa, T. Nanocomposite Hydrogels: A Unique Organic−Inorganic Network Structure with Extraordinary Mechanical, Optical, and Swelling/De-swelling Properties. *Adv. Mater.* **2002**, *14*, 1120−1124.
(47) Haraguchi, K.; Takehisa, T.; Fan, S. Effects of Clay Content on the Properties of Nanocomposite Hydrogels Composed of Poly(N-isopropylacrylamide) and Clay. *Macromolecules* **2002**, *35*, 10162−10171.